Nonlinear Analysis: Modelling and Control, Online First, 1–18
https://doi.org/10.15388/namc.2025.30.43746

Vilnius University Press

Arnold tongues of divergence in the Caputo fractional standard map of nilpotent matrices*

Ugnė Orinaitė, Rasa Šmidtaitė, Minvydas Ragulskis

Research Group for Nonlinear Systems, Kaunas University of Technology,
Studentų 50-146, Kaunas LT-51368, Lithuania

ugne.orinaite@ktu.lt; rasa.smidtaite@ktu.lt; minvydas.ragulskis@ktu.lt

Received: April 5, 2025 / **Revised:** July 15, 2025 / **Published online:** October 7, 2025

Abstract. Arnold tongues of divergence in the Caputo fractional standard map of nilpotent matrices are explored in this paper. The scalar iterative variables in the Caputo fractional standard map are replaced by iterative matrix variables. The divergence effects induced by the nilpotent matrices result in specific patterns of Arnold tongues. Automatic machine classification techniques help to identify different types of Arnold tongues according to the dynamics of the transient processes of the system. Computational experiments are used to validate theoretical insights and to reveal the patterns of Arnold tongues of divergence.

Keywords: Arnold tongue, Caputo fractional standard map, nilpotent, divergence.

1 Introduction

Fractional calculus, which generalizes traditional integer-order calculus by allowing derivatives and integrals of noninteger order, has been widely adopted in the study of complex systems due to its ability to capture nonlocal, memory-dependent dynamics. Fractional derivatives have proven beneficial in modeling systems, where the future state depends not only on the current state but also on a continuum of past states. Fractional derivatives are often defined through the Caputo or Riemann–Liouville formulations [2] and have found applications across diverse fields, such as viscoelasticity, anomalous diffusion, and electrical circuits [15, 17].

The standard map, also known as the Chirikov–Taylor map [3, 4], has served as a fundamental tool in exploring the transition from regular to chaotic motion in Hamiltonian systems. Originally developed to model particle dynamics in magnetic fields, this discrete-time, area-preserving map represents a simplified system that captures the essence of chaotic behavior in nonlinear systems. The utility of a standard map to visualize bifurcation scenarios and resonances is illustrated in [23].

*This work is supported by Students' research project No. S-ST-24-11 founded by Research Council of Lithuania.

For the first time, the fractional standard map was derived from fractional differential equation with Caputo and Riemann–Liouville fractional derivative in [31]. The generalization of Caputo fractional standard map on arbitrary orders of Caputo and Riemann–Liouville fractional derivatives are proposed in [24–26]. The first computer simulation of the fractional standard map is realized in [10, 30].

Arnold tongues, named after the mathematician Vladimir Arnold [1], represent parameter regions in dynamical systems, where the phase-locking or resonance occurs. These structures are crucial in systems with periodic driving, as they indicate ranges, where the system's response locks onto rational rotation numbers.

The complexity of a discrete-time system can be increased not only by adding new spatial elements (resulting into coupled map lattices) but also by increasing the dimensionality of a node. Replacing a scalar variable in a classical logistic map by a square two-dimensional matrix introduces unexpected phenomena, such as finite-time and explosive divergence [19]. The effect of explosive divergence in the logistic map of matrices occurs when the Lyapunov exponent of the scalar logistic map becomes positive. Such behavior is not limited to logistic map of matrices and is typical to a discrete system of matrices if the mapping function is analytic [18].

The main objective of this study is to explore the Caputo fractional standard map with scalar iterative variables replaced by matrix iterative variables. While the scalar Caputo fractional standard map provides insight into chaotic behavior of fractional systems, the matrix extension of the model enables the exploration of more complex dynamical behaviors. In particular, the major interest is focused on the effects induced by the matrix variables (the finite-time and explosive divergence). How those effects may change the properties of the Arnold tongues observed in the scalar Caputo fractional standard map is the main question raised in this paper. This paper aims to further enrich the theoretical framework of Caputo fractional systems, contributing both to the fractional calculus applied for nonlinear dynamical systems and to the real-world applications that require modeling of complex multidimensional systems.

This manuscript is structured as follows. Section 2 discusses the preliminary concepts required for this research. The Caputo fractional standard map of matrices is formulated in Section 3, exploring the complex dynamics induced by idempotent and nilpotent matrices. Section 4 focuses on the use of H-ranks to identify Arnold tongues and their relevance in the Caputo fractional standard map. Section 5 introduces a novel approach to classifying transient processes using k-means clustering. Discussion and concluding remarks are given in Section 6.

2 Preliminaries

2.1 The universal map

Let us consider the universal equation of motion [31]

$$\ddot{x}(t) + KG\big[x(t)\big] \sum_{k=1}^{\infty} \delta\left(\frac{t}{T} - k\right) = 0, \tag{1}$$

where perturbation is a delta-function-type kick with period T, K is an amplitude of a pulse, and $G(x)$ is a real-valued function. This equation can be represented in the Hamiltonian form:

$$\dot{p} + KG(x)\sum_{k=1}^{\infty}\delta\left(\frac{t}{T}-k\right)=0, \qquad \dot{x}=p.$$

It is well known that this equation can be represented in the form of discrete map [37]:

$$\begin{aligned} p^{(k+1)} &= p^{(k)} - KTG\big(x^{(k)}\big),\\ x^{(k+1)} &= x^{(k)} + Tp^{(k+1)}. \end{aligned}$$

If function $G(x) = \sin x$ (with period $T = 1$), the standard Chirikov–Taylor map is obtained [4]:

$$\begin{aligned} p^{(k+1)} &= p^{(k)} - K\sin x^{(k)},\\ x^{(k+1)} &= x^{(k)} + p^{(k+1)}. \end{aligned}$$

2.2 Fractional generalization of the universal map and the standard map

Let us consider a fractional generalization of differential equation (1) [25]

$${}_0^C D_t^{\alpha} x(t) + KG\big[x(t)\big]\sum_{j=1}^{\infty}\delta\left(\frac{t}{T}-j\right)=0, \tag{2}$$

where α is the order of fractional derivative, $m-1<\alpha<m$; ${}_0^C D_t^{\alpha}$ is the Caputo fractional derivative with the initial conditions

$${}_0^C D_t^{s} x(0) = \big(D_t^{s} x\big)(0) = {}^{(s)}x^{(0)},$$

where $s = 0, 1, \ldots, m-1$. This Cauchy-type problem for fractional differential equations (2) is equivalent to the discrete map equations [25]

$$\begin{aligned} {}^{(s)}x^{(k+1)} = {}& \sum_{j=0}^{m-s-1}\frac{{}^{(j+s)}x^{(0)}}{j!}(k+1)^j T^j\\ & - \frac{KT^{\alpha-s}}{\Gamma(\alpha-s)}\sum_{j=1}^{k}(k+1-j)^{\alpha-1-s}G\big(x^{(j)}\big). \end{aligned}$$

Let us note that if the fractional order $1<\alpha<2$ and notations of $p^{(k)} = {}^{(1)}x^{(k)}$ and $x^{(k)} = {}^{(0)}x^{(k)}$ are introduced, then the map is expressed as

$$p^{(k+1)} = p^{(0)} - \frac{KT^{\alpha-1}}{\Gamma(\alpha-1)}\sum_{j=1}^{k}(k+1-j)^{\alpha-2}G\big(x^{(j)}\big),$$

$$x^{(k+1)} = x^{(0)} + (k+1)Tp^{(0)} - \frac{KT^{\alpha}}{\Gamma(\alpha)}\sum_{j=1}^{k}(k+1-j)^{\alpha-1}G\big(x^{(j)}\big).$$

If the function $G(x) = \sin x$ and period T is set to 1, then the following Caputo fractional standard map ($1 < \alpha < 2$) is obtained:

$$p^{(k+1)} = p^{(0)} - \frac{K}{\Gamma(\alpha-1)} \sum_{j=1}^{k} (k+1-j)^{\alpha-2} \sin x^{(j)} \pmod{2\pi},$$

$$x^{(k+1)} = x^{(0)} + (k+1)p^{(0)} - \frac{K}{\Gamma(\alpha)} \sum_{j=1}^{k} (k+1-j)^{\alpha-1} \sin x^{(j)} \pmod{2\pi}.$$

The introduction of $V_\alpha^s(m)$ helps to reduce the Caputo fractional standard map to a more common form [6, 20]:

$$\begin{aligned} p^{(k+1)} &= p^{(k)} - \frac{K}{\Gamma(\alpha-1)} \left(\sum_{j=0}^{k-1} V_\alpha^2(k-j+1) \sin x^{(j)} + \sin x^{(k)} \right) \pmod{2\pi}, \\ x^{(k+1)} &= x^{(k)} + p^{(0)} - \frac{K}{\Gamma(\alpha)} \sum_{j=0}^{k} V_\alpha^1(k-j+1) \sin x^{(j)} \pmod{2\pi}, \end{aligned} \tag{3}$$

where $k = 0, 1, 2, \ldots$, K is the parameter of the standard map, α is the fractionality parameter ($1 < \alpha \leqslant 2$), and

$$V_\alpha^s(m) = m^{\alpha-s} - (m-1)^{\alpha-s}, \quad m = 1, 2, \ldots .$$

Note that the summation $\sum_{j=0}^{k-1} V_\alpha^2(k-j+1) \sin x^{(j)}$ in Eq. (3) is not executed at $k = 0$ ($p^{(1)} = p^{(0)} - K \sin x^{(0)}/\Gamma(\alpha-1) \pmod{2\pi}$). Usually, $x^{(0)}$ is set to 0 [6].

2.3 Idempotents and nilpotents

Let us consider a square matrix $\mathbf{X} \in \mathbb{R}^{2\times 2}$ and its eigenvalues $\lambda_1, \lambda_2 \in \mathbb{R}$.

$\mathbf{X}$ can be expressed in the form comprising conjugate idempotents if $\lambda_1 \neq \lambda_2$:

$$\mathbf{X} = \lambda_1 \mathbf{D}_1 + \lambda_2 \mathbf{D}_2.$$

Here $\mathbf{D}_1, \mathbf{D}_2 \in \mathbb{R}^{2\times 2}$ are conjugate idempotents ($\mathbf{D}_1 + \mathbf{D}_2 = \mathbf{I}$, where $\mathbf{I}$ denotes the identity matrix) satisfying the following properties:

$$\det \mathbf{D}_1 = \det \mathbf{D}_2 = 0, \qquad (\mathbf{D}_1)^2 = \mathbf{D}_1,$$
$$(\mathbf{D}_2)^2 = \mathbf{D}_2, \qquad \mathbf{D}_1\mathbf{D}_2 = \mathbf{D}_2\mathbf{D}_1 = \Theta,$$

where Θ is the null matrix.

Otherwise (if $\lambda_1 = \lambda_2 := \lambda_0$), $\mathbf{X}$ can be expressed in the form comprising a nilpotent:

$$\mathbf{X} = \lambda_0 \mathbf{I} + \mu \mathbf{N},$$

where $\mu \in \mathbb{R}$, $\mathbf{N} = \mathbf{T} \left[\begin{smallmatrix} 0 & 1 \\ 0 & 0 \end{smallmatrix}\right] \mathbf{T}^{-1}$, $\mathbf{T} \in \mathbb{R}^{2\times 2}$, $\det \mathbf{T} \neq 0$, and $\mathbf{N}$ is a nilpotent satisfying the following relationships:

$$\det \mathbf{N} = 0, \qquad \mathbf{N}^2 = \Theta.$$

3 The Caputo fractional standard map of matrices

Scalar variables $x^{(k)}$ and $p^{(k)}$ in Eq. (3) can be replaced by the square matrices

$$\mathbf{X}^{(k)} = \begin{bmatrix} x_{11}^{(k)} & x_{12}^{(k)} \\ x_{21}^{(k)} & x_{22}^{(k)} \end{bmatrix}, \quad x_{11}^{(k)}, x_{12}^{(k)}, x_{21}^{(k)}, x_{22}^{(k)} \in \mathbb{R},$$

and

$$\mathbf{P}^{(k)} = \begin{bmatrix} p_{11}^{(k)} & p_{12}^{(k)} \\ p_{21}^{(k)} & p_{22}^{(k)} \end{bmatrix}, \quad p_{11}^{(k)}, p_{12}^{(k)}, p_{21}^{(k)}, p_{22}^{(k)} \in \mathbb{R}.$$

Then the discrete map of matrices reads

$$\mathbf{P}^{(k+1)} = \mathbf{P}^{(k)} - \frac{K}{\Gamma(\alpha-1)} \left(\sum_{j=0}^{k-1} V_\alpha^2(k-j+1) \sin \mathbf{X}^{(j)} + \sin \mathbf{X}^{(k)} \right) \pmod{2\pi},$$

$$\mathbf{X}^{(k+1)} = \mathbf{X}^{(k)} + \mathbf{P}^{(0)} - \frac{K}{\Gamma(\alpha)} \sum_{j=0}^{k} V_\alpha^1(k-j+1) \sin \mathbf{X}^{(j)} \pmod{2\pi},$$

where $k = 0, 1, 2, \ldots$.

3.1 The Caputo fractional standard map of idempotent matrices

Corollary 1. *Let* $\mathbf{P}^{(0)} = c_1\mathbf{D}_1 + c_2\mathbf{D}_2$, *where* $\mathbf{D}_1$ *and* $\mathbf{D}_2$ *are conjugate idempotents, and* $c_1, c_2 \in \mathbb{R}$. *Then*

$$\sin \mathbf{P}^{(0)} = \sin(c_1)\mathbf{D}_1 + \sin(c_2)\mathbf{D}_2.$$

Proof.

$$\begin{aligned}
\sin \mathbf{P}^{(0)} &= \sum_{j=0}^{\infty} \frac{(-1)^j}{(2j+1)!} (c_1\mathbf{D}_1 + c_2\mathbf{D}_2)^{2j+1} \\
&= \sum_{j=0}^{\infty} \frac{(-1)^j}{(2j+1)!} \left(\binom{2j+1}{0} (c_1)^{2j+1} (\mathbf{D}_1)^{2j+1} \right. \\
&\quad + \binom{2j+1}{1} (c_1)^{2j} c_2 (\mathbf{D}_1)^{2j} \mathbf{D}_2 + \cdots + \binom{2j+1}{2j} c_1 (c_2)^{2j} \mathbf{D}_1 (\mathbf{D}_2)^{2j} \\
&\quad \left. + \binom{2j+1}{2j+1} (c_2)^{2j+1} (\mathbf{D}_2)^{2j+1} \right) \\
&= \sum_{j=0}^{\infty} \frac{(-1)^j}{(2j+1)!} \left((c_1)^{2j+1}\mathbf{D}_1 + (c_2)^{2j+1}\mathbf{D}_2 \right) \\
&= \sin(c_1)\mathbf{D}_1 + \sin(c_2)\mathbf{D}_2.
\end{aligned}$$

□

Lemma 1. *Let the matrices of initial conditions* $\mathbf{P}^{(0)}$ *and* $\mathbf{X}^{(0)}$ *be idempotent matrices with the same conjugate idempotents*:

$$\mathbf{P}^{(0)} = \lambda_{1,p}^{(0)}\mathbf{D}_1 + \lambda_{2,p}^{(0)}\mathbf{D}_2 \quad \textit{and} \quad \mathbf{X}^{(0)} = \lambda_{1,x}^{(0)}\mathbf{D}_1 + \lambda_{2,x}^{(0)}\mathbf{D}_2, \quad \lambda_{1,x}^{(0)}, \lambda_{2,x}^{(0)} \in \mathbb{R},$$

where $\lambda_{1,x}^{(0)}, \lambda_{2,x}^{(0)} \neq 0$. *Then iterative matrices* $\mathbf{P}^{(k+1)}$ *and* $\mathbf{X}^{(k+1)}$ $(k = 0, 1, 2, \dots)$ *are also idempotent matrices with the same conjugate idempotents* $\mathbf{D}_1$ *and* $\mathbf{D}_2$.

Proof. Let us suppose that $\mathbf{P}^{(k)} = \lambda_{1,p}^{(k)}\mathbf{D}_1 + \lambda_{2,p}^{(k)}\mathbf{D}_2$ and $\mathbf{X}^{(k)} = \lambda_{1,x}^{(k)}\mathbf{D}_1 + \lambda_{2,x}^{(k)}\mathbf{D}_2$. Then

$$\begin{aligned}
\mathbf{P}^{(k+1)} &= \mathbf{P}^{(k)} - \frac{K}{\Gamma(\alpha-1)}\left(\sum_{j=0}^{k-1} V_\alpha^2(k-j+1)\sin\mathbf{X}^{(j)} + \sin\mathbf{X}^{(k)}\right)\\
&= \left(\lambda_{1,p}^{(k)}\mathbf{D}_1 + \lambda_{2,p}^{(k)}\mathbf{D}_2\right)\\
&\quad - \frac{K}{\Gamma(\alpha-1)}\left(\sum_{j=0}^{k-1} V_\alpha^2(k-j+1)\sin\left(\lambda_{1,x}^{(j)}\mathbf{D}_1 + \lambda_{2,x}^{(j)}\mathbf{D}_2\right)\right.\\
&\quad \left. + \sin\left(\lambda_{1,x}^{(k)}\mathbf{D}_1 + \lambda_{2,x}^{(k)}\mathbf{D}_2\right)\right)\\
&= \left(\lambda_{1,p}^{(k)} - \frac{K}{\Gamma(\alpha-1)}\left(\sum_{j=0}^{k-1} V_\alpha^2(k-j+1)\sin\lambda_{1,x}^{(j)} + \sin\lambda_{1,x}^{(k)}\right)\right)\mathbf{D}_1\\
&\quad + \left(\lambda_{2,p}^{(k)} - \frac{K}{\Gamma(\alpha-1)}\left(\sum_{j=0}^{k-1} V_\alpha^2(k-j+1)\sin\lambda_{2,x}^{(j)} + \sin\lambda_{2,x}^{(k)}\right)\right)\mathbf{D}_2 \pmod{2\pi},\\
\mathbf{X}^{(k+1)} &= \mathbf{X}^{(k)} + \mathbf{P}^{(0)} - \frac{K}{\Gamma(\alpha)}\sum_{j=0}^{k} V_\alpha^1(k-j+1)\sin\mathbf{X}^{(j)}\\
&= \left(\lambda_{1,x}^{(k)}\mathbf{D}_1 + \lambda_{2,x}^{(k)}\mathbf{D}_2\right) + \left(\lambda_{1,p}^{(0)}\mathbf{D}_1 + \lambda_{2,p}^{(0)}\mathbf{D}_2\right)\\
&\quad - \frac{K}{\Gamma(\alpha)}\sum_{j=0}^{k} V_\alpha^1(k-j+1)\sin\left(\lambda_{1,x}^{(j)}\mathbf{D}_1 + \lambda_{2,x}^{(j)}\mathbf{D}_2\right)\\
&= \left(\lambda_{1,x}^{(k)} + \lambda_{1,p}^{(0)} - \frac{K}{\Gamma(\alpha)}\sum_{j=0}^{k} V_\alpha^1(k-j+1)\sin\lambda_{1,x}^{(j)}\right)\mathbf{D}_1\\
&\quad + \left(\lambda_{2,x}^{(k)} + \lambda_{2,p}^{(0)} - \frac{K}{\Gamma(\alpha)}\sum_{j=0}^{k} V_\alpha^1(k-j+1)\sin\lambda_{2,x}^{(j)}\right)\mathbf{D}_2 \pmod{2\pi}. \qquad \square
\end{aligned}$$

Lemma 1 implies that the Caputo fractional standard map of idempotent matrices splits into four scalar maps of eigenvalues representing two uncoupled scalar Caputo

fractional standard maps:

$$\begin{aligned}
\lambda_{1,p}^{(k+1)} &= \lambda_{1,p}^{(k)} - \frac{K}{\Gamma(\alpha-1)}\left(\sum_{j=0}^{k-1} V_\alpha^2(k-j+1)\sin\lambda_{1,x}^{(j)} + \sin\lambda_{1,x}^{(k)}\right) \pmod{2\pi},\\
\lambda_{1,x}^{(k+1)} &= \lambda_{1,x}^{(k)} + \lambda_{1,p}^{(0)} - \frac{K}{\Gamma(\alpha)}\sum_{j=0}^{k} V_\alpha^1(k-j+1)\sin\lambda_{1,x}^{(j)} \pmod{2\pi},\\
\lambda_{2,p}^{(k+1)} &= \lambda_{2,p}^{(k)} - \frac{K}{\Gamma(\alpha-1)}\left(\sum_{j=0}^{k-1} V_\alpha^2(k-j+1)\sin\lambda_{2,x}^{(j)} + \sin\lambda_{2,x}^{(k)}\right) \pmod{2\pi},\\
\lambda_{2,x}^{(k+1)} &= \lambda_{2,x}^{(k)} + \lambda_{2,p}^{(0)} - \frac{K}{\Gamma(\alpha)}\sum_{j=0}^{k} V_\alpha^1(k-j+1)\sin\lambda_{2,x}^{(j)} \pmod{2\pi},
\end{aligned} \tag{4}$$

where $k = 0, 1, 2, \dots$. In other words, the complexity of the Caputo fractional standard map of idempotent matrices is exactly the same as the complexity of the scalar Caputo fractional standard map.

3.2 The Caputo fractional standard map of nilpotent matrices

Corollary 2. *Let* $\mathbf{P}^{(0)} = c_0\mathbf{I} + c_1\mathbf{N}$*, where* $c_0, c_1 \in \mathbb{R}$*,* $c_1 \neq 0$*. Then*

$$\sin\mathbf{P}^{(0)} = \sin(c_0)\mathbf{I} + \cos(c_0)c_1\mathbf{N}.$$

Proof.

$$\begin{aligned}
\sin\mathbf{P}^{(0)} &= \sum_{j=0}^{\infty}\frac{(-1)^j}{(2j+1)!}(c_0\mathbf{I} + c_1\mathbf{N})^{2j+1}\\
&= \sum_{j=0}^{\infty}\frac{(-1)^j}{(2j+1)!}\left(\binom{2j+1}{0}(c_0)^{2j+1}\mathbf{I}^{2j+1} + \binom{2j+1}{1}(c_0)^{2j}c_1\mathbf{I}^{2j}\mathbf{N}\right.\\
&\quad \left. + \cdots + \binom{2j+1}{2j}c_0(c_1)^{2j}\mathbf{I}(\mathbf{N})^{2j} + \binom{2j+1}{2j+1}(c_1)^{2j+1}(\mathbf{N})^{2j+1}\right)\\
&= \left(\sum_{j=0}^{\infty}\frac{(-1)^j}{(2j+1)!}(c_0)^{2j+1}\right)\mathbf{I} + \left(\sum_{j=0}^{\infty}\frac{(-1)^j}{(2j+1)!}(2j+1)(c_0)^{2j}\right)c_1\mathbf{N}\\
&= \left(\sum_{j=0}^{\infty}\frac{(-1)^j}{(2j+1)!}(c_0)^{2j+1}\right)\mathbf{I} + (\sum_{j=0}^{\infty}\frac{(-1)^j}{(2j)!}(c_0)^{2j})c_1\mathbf{N}\\
&= \sin(c_0)\mathbf{I} + \cos(c_0)c_1\mathbf{N}, \quad k = 0, 1, 2, \dots .
\end{aligned}$$

□

Lemma 2. *Let the matrices of initial conditions* $\mathbf{P}^{(0)}$ *and* $\mathbf{X}^{(0)}$ *share the same nilpotent*:

$$\mathbf{P}^{(0)} = \lambda_p^{(0)}\mathbf{I} + \mu_p^{(0)}\mathbf{N} \quad \textit{and} \quad \mathbf{X}^{(0)} = \lambda_x^{(0)}\mathbf{I} + \mu_x^{(0)}\mathbf{N}, \quad \lambda_p^{(0)}, \lambda_x^{(0)}, \mu_p^{(0)}, \mu_x^{(0)} \in \mathbb{R},$$

where $\mu_p^{(0)}, \mu_x^{(0)} \neq 0$*. Then iterative matrices* $\mathbf{P}^{(k+1)}$ *and* $\mathbf{X}^{(k+1)}$ $(k = 0, 1, 2, \dots)$ *also share the same nilpotent* $\mathbf{N}$*.*

Proof. Let us suppose that $\mathbf{P}^{(k)} = \lambda_p^{(k)}\mathbf{I} + \mu_p^{(k)}\mathbf{N}$ and $\mathbf{X}^{(k)} = \lambda_x^{(k)}\mathbf{I} + \mu_x^{(k)}\mathbf{N}$. Then

$$
\begin{aligned}
&\mathbf{P}^{(k+1)}\\
&\quad= \mathbf{P}^{(k)} - \frac{K}{\Gamma(\alpha-1)}\left(\sum_{j=0}^{k-1} V_\alpha^2(k-j+1)\sin\mathbf{X}^{(j)} + \sin\mathbf{X}^{(k)}\right)\\
&\quad= \big(\lambda_p^{(k)}\mathbf{I} + \mu_p^{(k)}\mathbf{N}\big) - \frac{K}{\Gamma(\alpha-1)}\left(\sum_{j=0}^{k-1} V_\alpha^2(k-j+1)\sin\big(\lambda_x^{(j)}\mathbf{I} + \mu_x^{(j)}\mathbf{N}\big)\right.\\
&\qquad\left.+ \sin\big(\lambda_x^{(k)}\mathbf{I} + \mu_x^{(k)}\mathbf{N}\big)\right)\\
&\quad= \left(\lambda_p^{(k)} - \frac{K}{\Gamma(\alpha-1)}\left(\sum_{j=0}^{k-1} V_\alpha^2(k-j+1)\sin\lambda_x^{(j)} + \sin\lambda_x^{(k)}\right)\right)\mathbf{I}\\
&\qquad+ \left(\mu_p^{(k)} - \frac{K}{\Gamma(\alpha-1)}\left(\sum_{j=0}^{k-1} V_\alpha^2(k-j+1)\mu_x^{(j)}\cos\lambda_x^{(j)}\right.\right.\\
&\qquad\left.\left.+ \mu_x^{(k)}\cos\lambda_x^{(k)}\right)\right)\mathbf{N} \pmod{2\pi},
\end{aligned}
\tag{5}
$$

$$
\begin{aligned}
&\mathbf{X}^{(k+1)}\\
&\quad= \mathbf{X}^{(k)} + \mathbf{P}^{(0)} - \frac{K}{\Gamma(\alpha)}\sum_{j=0}^{k} V_\alpha^1(k-j+1)\sin\mathbf{X}^{(j)}\\
&\quad= \big(\lambda_x^{(k)}\mathbf{I} + \mu_x^{(k)}\mathbf{N}\big) + \big(\lambda_p^{(0)}\mathbf{I} + \mu_p^{(0)}\mathbf{N}\big)\\
&\qquad- \frac{K}{\Gamma(\alpha)}\sum_{j=0}^{k} V_\alpha^1(k-j+1)\sin\big(\lambda_x^{(j)}\mathbf{I} + \mu_x^{(j)}\mathbf{N}\big)\\
&\quad= \left(\lambda_x^{(k)} + \lambda_p^{(0)} - \frac{K}{\Gamma(\alpha)}\sum_{j=0}^{k} V_\alpha^1(k-j+1)\sin\lambda_x^{(j)}\right)\mathbf{I}\\
&\qquad+ \left(\mu_x^{(k)} + \mu_p^{(0)} - \frac{K}{\Gamma(\alpha)}\sum_{j=0}^{k} V_\alpha^1(k-j+1)\mu_x^{(j)}\cos\lambda_x^{(j)}\right)\mathbf{N} \pmod{2\pi}.
\end{aligned}
$$

The proof is complete. □

Lemma 2 implies that Eq. (5) splits into two intertwined scalar maps of the eigenvalues $\lambda_p^{(k)}$, $\lambda_x^{(k)}$ and the auxiliary parameters $\mu_p^{(k)}$, $\mu_x^{(k)}$:

$$
\begin{aligned}
\lambda_p^{(k+1)} &= \lambda_p^{(k)} - \frac{K}{\Gamma(\alpha-1)}\left(\sum_{j=0}^{k-1} V_\alpha^2(k-j+1)\sin\lambda_x^{(j)} + \sin\lambda_x^{(k)}\right) \pmod{2\pi},\\
\lambda_x^{(k+1)} &= \lambda_x^{(k)} + \lambda_p^{(0)} - \frac{K}{\Gamma(\alpha)}\sum_{j=0}^{k} V_\alpha^1(k-j+1)\sin\lambda_x^{(j)} \pmod{2\pi},
\end{aligned}
\tag{6$_1$}
$$

$$\begin{aligned}\mu_p^{(k+1)} &= \mu_p^{(k)} - \frac{K}{\Gamma(\alpha-1)}\left(\sum_{j=0}^{k-1} V_\alpha^2(k-j+1)\mu_x^{(j)}\cos\lambda_x^{(j)} + \mu_x^{(k)}\cos\lambda_x^{(k)}\right),\\ \mu_x^{(k+1)} &= \mu_x^{(k)} + \mu_p^{(0)} - \frac{K}{\Gamma(\alpha)}\sum_{j=0}^{k} V_\alpha^1(k-j+1)\mu_x^{(j)}\cos\lambda_x^{(j)},\end{aligned} \tag{6$_2$}$$

where $k = 0, 1, 2, \ldots$. In other words, the complexity of Eq. (5) becomes very much different compared to the complexity of the scalar Caputo fractional standard map.

Definition 1. The iterative model (6) is denoted as the Caputo fractional standard map of nilpotent matrices.

4 H-ranks for the identification of Arnold tongues

H-ranks are successfully used to quantify the complexity of the scalar Caputo fractional standard map when the fractionality parameter α changes from 2 to 1 (the ornament of Arnold tongues does emerge in the digital image of H-ranks as α tends to 1) [20]. A natural question is whether Arnold tongues also appear in the Caputo fractional standard map of idempotent matrices as α tends to 1.

The pattern of H-ranks computed for the scalar Caputo fractional standard map at $\alpha = 1.001$ is shown in Fig. 1(a). The initial condition $x^{(0)}$ is set to 0, while $p^{(0)} \in [0, 2\pi]$ and $K \in [0, 2]$ (Fig. 1(a)). The maximum H-rank is set to 200 (the observation window for the computation of the H-rank comprises the first 399 elements of the sequence $\mu_x^{(k)}$, $k = 0, 1, \ldots, 398$, for each value of $p^{(0)}$ and K.

Computational experiments are continued with the Caputo fractional standard map of nilpotent matrices at $\alpha = 1.001$. The initial conditions are set as follows: $\lambda_x^{(0)} = 0$, $\mu_p^{(0)} = 1$, $\mu_x^{(0)} = 1$, while $\lambda_p^{(0)} \in [0, 2\pi]$ and $K \in [0, 2]$ (Fig. 1(b)). It is rather astonishing to observe that the ornaments of the Arnold tongues in Figs. 1(a) and 1(b) are almost identical.

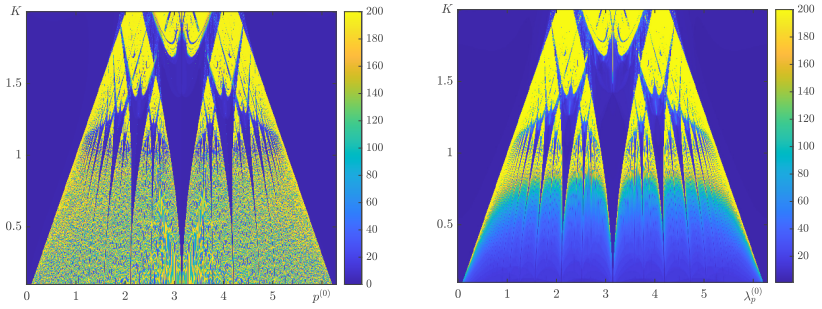

Figure 1. The pattern of H-ranks for the scalar Caputo fractional standard map (panel (a)) and Caputo fractional standard map of nilpotent matrices (panel (b)). Initial conditions for scalar map (panel (a)) are set to $\alpha = 1.001$, $x^{(0)} = 0$, $p^{(0)} \in [0, 2\pi]$, $K \in [0, 2]$. Initial conditions for map of nilpotent matrices (panel (b)) are set to $\alpha = 1.001$, $\lambda_x^{(0)} = 0$, $\mu_p^{(0)} = 1$, $\mu_x^{(0)} = 1$, $\lambda_p^{(0)} \in [0, 2\pi]$, $K \in [0, 2]$.

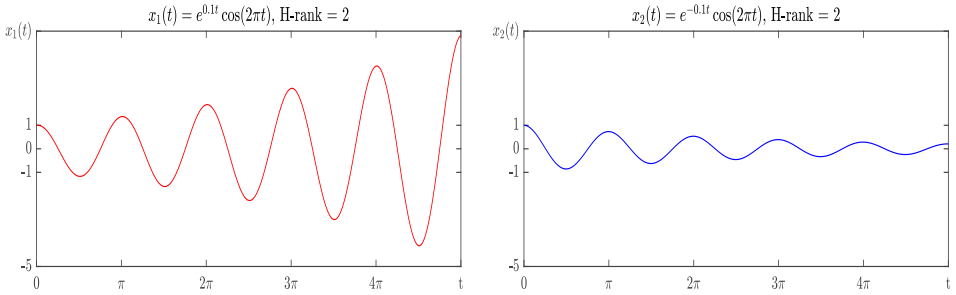

Figure 2. The H-ranks computed for two different time series $x_1(t) = \exp(0.1t)\cos(2\pi t)$ (panel (a)) and $x_1(t) = \exp(-0.1t)\cos(2\pi t)$ (panel (b)). The behavior of these functions is different, although the H-ranks are equal.

It is well known that the introduction of matrix iterative variables instead of scalar iterative variables may introduce finite-time or even explosive divergence of the originally stable system [35]. Also, it is known that periodic orbits do not exist in the fractional-order models (discrete or continuous), except for fixed points [13, 32–34, 36]. And although an exact periodic motion is not possible, the asymptotically periodic solutions may be present in fractional-order systems [7–9, 11, 22]. Therefore, the similarity of the Arnold tongues in Figs. 1(a) and 1(b) is an even more unexpected phenomenon, which can be explained by the implications induced by the "no-free-lunch theorems" [35]. In other words, each algorithm (including the H-rank algorithm) should be used with understanding of its limitations.

The H-rank algorithm is based on the identification of the number of algebraic components needed to approximate the given sequence with a predefined precision [21]. However, the type of algebraic components (in terms of its convergence or divergence) is not considered by the H-rank algorithm.

This effect is illustrated in Fig. 2. The H-ranks computed for two time series $x_1(t) = \exp(0.1t)\cos(2\pi t)$ (plotted in red) and $x_1(t) = \exp(-0.1t)\cos(2\pi t)$ (plotted in blue) are both equal to 2 (Fig. 2). This result is correct from an algebraic point of view. However, it is clear that the H-rank algorithm is not applicable for the detection of divergence processes induced by nilpotent matrices. This fact is explicitly illustrated in Fig. 3. It appears that H-ranks of the transient processes of $\mu_x^{(k)}$ at $\lambda_p^{(0)} = 1.73$ and $K = 1.12$ (Fig. 3(a)) and $\lambda_p^{(0)} = 5.40$ and $K = 1.41$ (Fig. 3(b)) are both equal to 64 (although the first transient process blows up, and the second quiets down).

A similar situation is illustrated in Fig. 3 panels (c) and (d). The transient process of $\mu_x^{(k)}$ blows up at $\lambda_p^{(0)} = 0.47$ and $K = 1.92$ (Fig. 3(c)) but yields a transient approach to an asymptotically periodic trajectory at $\lambda_p^{(0)} = 3.56$ and $K = 1.57$ (Fig. 3(d)). However, H-ranks of both transient processes are equal to 100 (Fig. 3).

Another argument against using the H-rank algorithm for the classification of different transient processes of $\mu_x^{(k)}$ is based on the limited size of the observation window. As mentioned previously, the maximum H-rank is set to 200 (resulting into the first 399 values of $\mu_x^{(k)}$ used to populate the catalectican Hankel matrix [20]). Larger observation

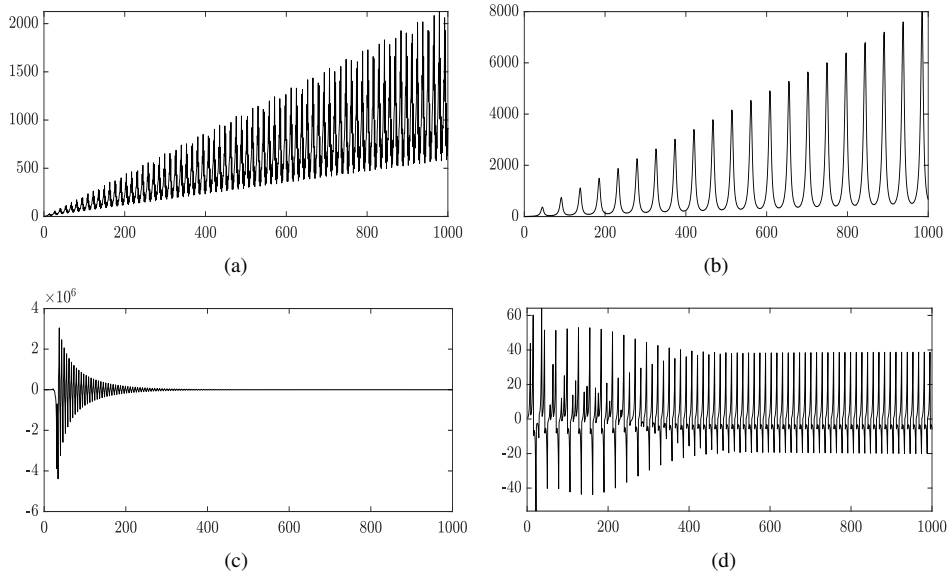

Figure 3. The transient dynamics of $\mu_x^{(k)}$: $p_{(0)} = 1.73$, $K = 1.12$, and H-rank is 64 (panel (a)); $p_{(0)} = 5.40$, $K = 1.41$, and H-rank is 64 (panel (b)); $p_{(0)} = 0.47$, $K = 1.92$, and H-rank is 100 (panel (c)); $p_{(0)} = 3.56$, $K = 1.57$, and H-rank is 100 (panel (d)).

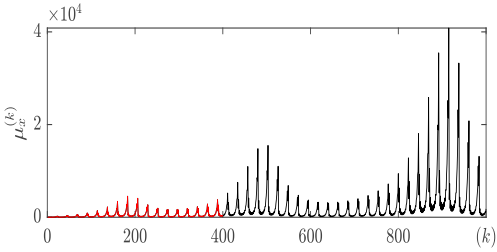

Figure 4. The transient dynamics of $\mu_x^{(k)}$ at $\mu_x^{(0)} = 1$, $\mu_p^{(0)} = 1$, $\lambda_x^{(0)} = 0$, $\lambda_p^{(0)} = 2.76$, and $K = 1.12$. The first 399 values of $\mu_x^{(k)}$ (plotted in red) are used to compute the H-rank of the sequence (H-rank is 197). Clearly, the first 399 values are not sufficient to describe the transient dynamics of $\mu_x^{(k)}$.

windows would yield into relatively large requirements for the computational hardware [20]. However, it appears that the Caputo fractional standard map of nilpotent matrices exhibits long transient processes (Fig. 4) and first 399 values of $\mu_x^{(k)}$ are not sufficient to describe the long-term dynamics of the system.

As already demonstrated in analytic and numerical simulations, nilpotent matrices can cause a rapid divergence of $\mu_x^{(k)}$, which would result in overflow after a sufficient number of iterations in time. One of the major objectives of this paper is to classify the dynamics of the transient trajectories of the Caputo fractional standard map of nilpotent matrices. The first 1000 values of $\mu_x^{(k)}$ are used for that purpose (Fig. 4). It appears that standard

double-precision floating-point arithmetic is sufficient for the Caputo fractional standard map of nilpotent matrices to avoid overflow (if only the number of iterations is limited to 1000).

5 Plotting Arnold tongues of divergence by using k-means clustering of PCA components

The classification of different transient processes produced by the Caputo fractional standard map of nilpotent matrices is performed using the k-means clustering algorithm [14]. To begin, the principal component analysis (PCA) is applied to the first 1000 values of $\mu_x^{(k)}$ to reduce the dimensionality of the data. The number of principal components retained in this step is selected based on the variance explained, ensuring that the reduced features capture the most significant variations in the data. Subsequently, the k-means clustering algorithm is applied to the reduced feature set. The classification results are visualized in Fig. 5(a) with 5 clusters and in Fig. 5(b) with 30 clusters, highlighting the impact of the chosen number of clusters on the classification outcome.

The essential difference between Fig. 1(b) and Fig. 5 is not only in the shape of Arnold tongues but also in the different types of Arnold tongues. Clearly, the H-rank algorithm is incapable of revealing those differences due to the reasons explained in the previous section.

The role of each individual class in Fig. 5 is explained by visualizing transient processes of $\mu_x^{(k)}$. For example, the two different points selected from the yellow zone in the $(\lambda_p^{(0)}, K)$-parameter plane show oscillating but diverging processes (Fig. 6). The two points chosen from the blue zone show processes, which quickly converge to the quiet state (Fig. 8). The two points selected from the orange zone result in transient approach to asymptotically periodic trajectories (Fig. 7). The two points taken from the green zone result in monotonously diverging trajectories (Fig. 9). Finally, the two points chosen from the light blue zone result into monotonous transient processes (Fig. 10).

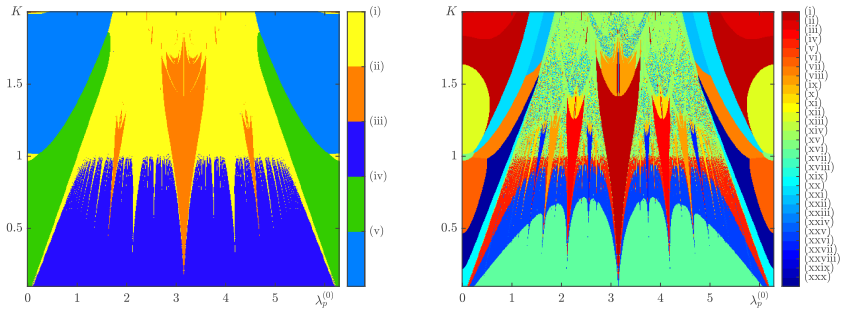

Figure 5. The classification of the transient processes of $\mu_x^{(k)}$ by using the k-means clustering algorithm on the reduced features. First 1000 values of $\mu_x^{(k)}$ at $\mu_x^{(0)} = 1$, $\mu_p^{(0)} = 1$, $\lambda_x^{(0)} = 0$, $\lambda_p^{(0)} \in [0, 2\pi]$, and $K \in [0, 2]$ are used for the classification. 5 different classes are used in panel (a); 30 classes are used in panel (b).

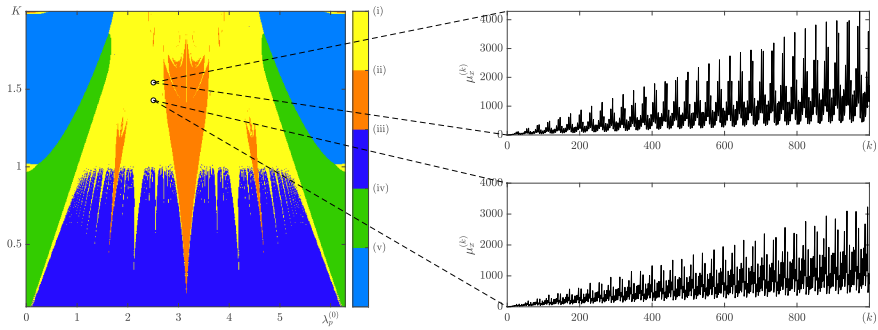

Figure 6. The classification of the transient processes of $\mu_x^{(k)}$ and pattern of Arnold tongues is shown in panel (a). The two different points selected from the yellow zone result into complex diverging processes as shown in panel (b).

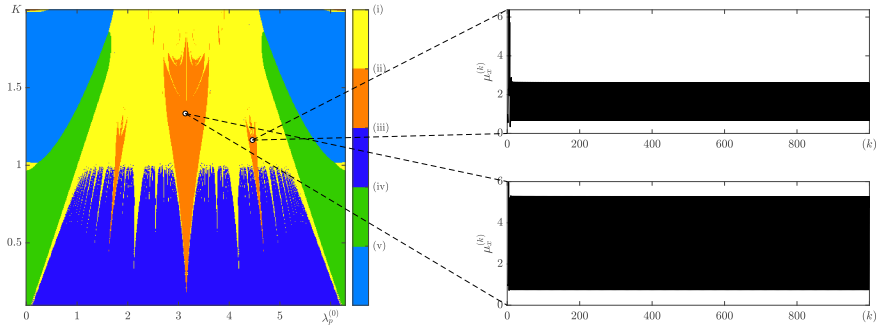

Figure 7. The classification of the transient processes of $\mu_x^{(k)}$ and pattern of Arnold tongues is shown in panel (a). The two different points selected from the orange zone result into oscillating processes with large amplitudes as shown in panel (b).

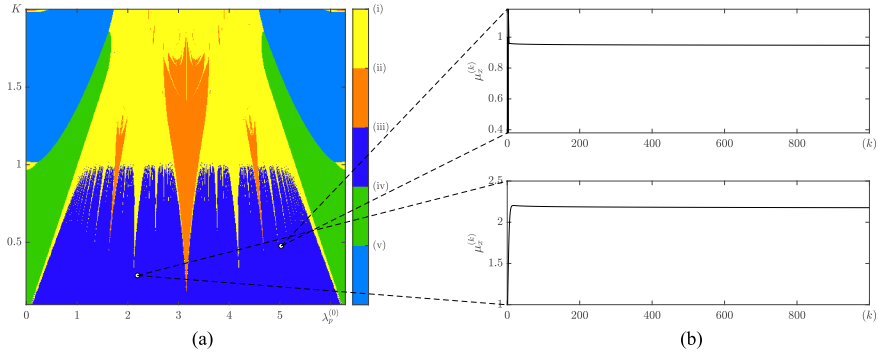

Figure 8. The classification of the transient processes of $\mu_x^{(k)}$ and pattern of Arnold tongues is shown in panel (a). The two different points selected from the blue zone result into a quick convergence to a quiet state as shown in panel (b).

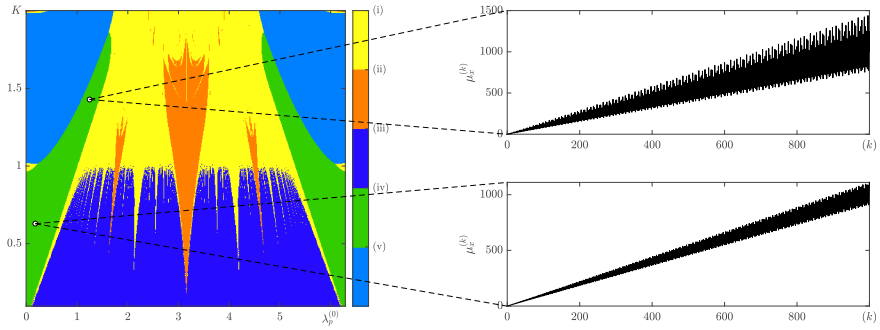

(a) (b)

Figure 9. The classification of the transient processes of $\mu_x^{(k)}$ and pattern of Arnold tongues is shown in panel (a). The two different points selected from the green zone result into oscillations with a linear diverging trend as shown in panel (b).

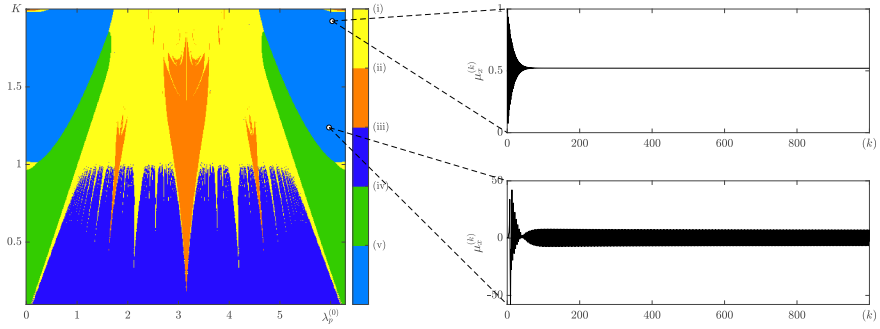

(a) (b)

Figure 10. The classification of the transient processes of $\mu_x^{(k)}$ and pattern of Arnold tongues is shown in panel (a). The two different points selected from the cyan zone result into relatively slow convergence to steady oscillations with a relatively small amplitude as shown in panel (b).

6 Discussion and concluding remarks

The concept of Arnold tongues of divergence in the Caputo fractional standard map of nilpotent matrices is introduced in this paper. It appears that the identification of Arnold tongues of divergence requires a proper adaptation of the computational techniques used for that purpose. A straightforward application of the standard H-rank algorithm fails to reveal the complexity of the emerging structure of Arnold tongues of divergence.

The fact of the existence of Arnold tongues in the Caputo fractional standard map is not unexpected. Some parallels could be drawn between the Caputo fractional standard map and the circle map [20], or even the paradigmatic Mathieu's equation [16]. For example, the region around the Arnold tongues in the time-periodic Mathieu's equation corresponds to the stable quasiperiod motion (the Arnold tongues correspond to the unstable exponential growth).

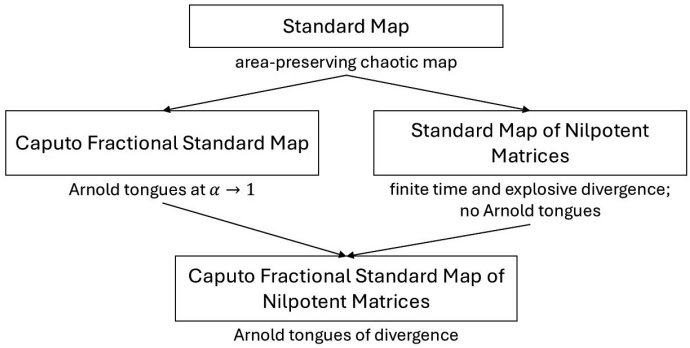

Figure 11. A schematic diagram illustrating the effects induced by fractional derivatives and nilpotent matrices.

A similar situation can be observed in Fig. 5. The dark blue region below the Arnold tongues corresponds to a stable quiet state (Fig. 8). The yellow region (including thin Arnold tongues) corresponds to complex diverging processes (Fig. 6). However, some of the Arnold tongues are orange (representing transient approach to asymptotically periodic trajectories in Fig. 7).

The situation becomes even more complex when the 30 classes are used to plot the colored representation of the Arnold tongues in Fig. 5(b). A more subtle classification reveals a much more complex structure of the Arnold tongues. The image in 5(b), though symmetric with respect to the central vertical axis, reveals the entire pallet of Arnold tongues plotted in different colors. Each tongue could be interpreted as a piano key producing a different sound. Each tongue shown in different color in Fig. 5(b) represents a slightly different transient process. It is worth mentioning that this variety of Arnold tongues is observable in the Caputo fractional standard map of nilpotent matrices. We call such tongues as Arnold tongues of divergence.

Arnold tongues of divergence are observable in Caputo fractional standard map of nilpotent matrices. Therefore, it is worth mentioning the basic properties of the standard map and its nonfractional and scalar counterparts (Fig. 11). As already mentioned in the Introduction, the paradigmatic standard map is firstly known as the area-preserving chaotic map. The introduction of fractional derivatives produces the scalar Caputo fractional standard map [5]. It is demonstrated in [20] that the Arnold tongue pattern emerges in the Caputo fractional standard map when the fractionality parameter α tends to 1.

As discussed in the Introduction, the replacement of the scalar iterative variable in a discrete chaotic map by the matrix iterative variable may result into the finite-time or even explosive divergence of the discrete map (if the matrix of initial conditions is a nilpotent matrix and the Lyapunov exponent of the scalar map is positive). However, such a replacement of the scalar iterative variable does not generate Arnold tongues in the standard map (Fig. 11). But Arnold tongues of divergence are generated by the Caputo fractional standard map of nilpotent matrices. Classical Arnold tongues in Caputo fractional standard map are transformed into Arnold tongues of divergence by the effects of finite-time and explosive divergence induced by nilpotent matrices.

This paper focuses on the study of nilpotent matrices but does not discuss other matrix types (such as idempotent matrices). The reason for ignoring idempotent matrices and their influence on Arnold tongues can be explained by the decomposition of model into decoupled scalar Caputo standard maps (Eq. (4)). Note that the formation of Arnold tongues in the scalar Caputo standard map is already investigated in [20].

Arnold tongues of divergence provide a much deeper insight into the dynamics of the system (compared to the paradigmatic Mathieu equation [12] and the scalar Caputo fractional standard map [20]). Arnold tongues of divergence do not only define regions of instability, where solutions grow exponentially, but also classify the divergent behavior of the system.

The dynamics of coupled Caputo fractional standard maps of nilpotent matrices remains an unexplored territory. Such fractional hypermaps of nilpotent matrices could open new directions for coding, hiding, and transmitting secret digital information, what is a definite objective of future research.

The article is limited to consideration only of maps that are derived from equations with Caputo fractional derivative. Different fractional maps are derived for the Riemann–Liouville [31], Erdélyi–Kober [29], Hadamard [28], and Hilfer [27] fractional derivatives. The exploration of the extended versions of such maps of nilpotent matrices also remains a clear objective of future research.

Author contributions. The authors (U.O., R.Š., and M.R.) have contributed as follows: software, investigation, visualization, U.O.; methodology, writing – original draft, investigation, R.S.; conceptualization, validation, supervision, M.R. All authors have read and approved the published version of the manuscript.

Conflicts of interest. The authors declare no conflicts of interest.

References

1. V.I. Arnol'd, Small denominators and problems of stability of motion in classical and celestial mechanics, *Russ. Math. Surv.*, **18**(6):85–191, 1963, https://doi.org/10.1070/RM1963v018n06ABEH001143.
2. E. Capelas de Oliveira, J.A. Tenreiro Machado, A review of definitions for fractional derivatives and integral, *Math. Probl. Eng.*, **2014**(1):238459, 2014, https://doi.org/10.1155/2014/238459.
3. B.V. Chirikov, Research concerning the theory of non-linear resonance and stochasticity, Report No. CERN-Trans-71-40, CERN, Geneva, 1971. Translated from Russian (original report: IYAF-267, Novosibirsk, 1969) by A.T. Sanders.
4. B.V. Chirikov, A universal instability of many-dimensional oscillator systems, *Phys. Rep.*, **52**(5):263–379, 1979, https://doi.org/10.1016/0370-1573(79)90023-1.
5. M. Edelman, Fractional standard map: Riemann–Liouville vs. Caputo, *Commun. Nonlinear Sci. Numer. Simul.*, **16**(12):4573–4580, 2011, https://doi.org/10.1016/j.cnsns.2011.02.007.

6. M. Edelman, Fractional maps as maps with power-law memory, in V. Afraimovich, A. Luo, X. Fu (Eds.), *Nonlinear Dynamics and Complexity*, Nonlinear Syst. Complex., Vol. 8, Springer, Cham, 2014, pp. 79–120, https://doi.org/10.1007/978-3-319-02353-3_3.
7. M. Edelman, Fractional maps and fractional attractors. Part II: Fractional difference Caputo α-families of maps, *Discontin. Nonlinearity Complex.*, **4**(4):391–402, 2015, https://doi.org/10.5890/DNC.2015.11.003.
8. M. Edelman, Periodic points, stability, bifurcations, and transition to chaos in generalized fractional maps, *IFAC-PapersOnLine*, **58**(12):131–142, 2024, ISSN 2405-8963, https://doi.org/10.1016/j.ifacol.2024.08.179. 12th IFAC Conference on Fractional Differentiation and its Applications ICFDA 2024
9. M. Edelman, A.B. Helman, R. Smidtaite, Bifurcations and transition to chaos in generalized fractional maps of the orders $0 < \alpha < 1$, *Chaos*, **33**(6):063123, 2023, https://doi.org/10.1063/5.0151812.
10. M. Edelman, V.E. Tarasov, Fractional standard map, *Phys. Lett. A*, **374**(2):279–285, 2009, https://doi.org/10.1016/j.physleta.2009.11.008.
11. H. He, W. Wang, Asymptotically periodic solutions of fractional order systems with applications to population models, *Appl. Math. Comput.*, **476**:128760, 2024, https://doi.org/10.1016/j.amc.2024.128760.
12. R.C. Hilborn, *Chaos and Nonlinear Dynamics: An Introduction for Scientists and Engineers,* 2 nd ed., Oxford Univ. Press, Oxford, 2000.
13. E. Kaslik, S. Sivasundaram, Non-existence of periodic solutions in fractional-order dynamical systems and a remarkable difference between integer and fractional-order derivatives of periodic functions, *Nonlinear Anal., Real World Appl.*, **13**(3):1489–1497, 2012, https://doi.org/10.1016/j.nonrwa.2011.11.013.
14. S. Lloyd, Least squares quantization in PCM, *IEEE Trans. Inf. Theory*, **28**(2):129–137, 1982, https://doi.org/10.1109/TIT.1982.1056489.
15. R.L. Magin, Fractional calculus in bioengineering, *Crit. Rev. Biomed. Eng.*, **32**(1):1–104, 2004, https://doi.org/10.1615/critrevbiomedeng.v32.i1.10.
16. É. Mathieu, Étude des solutions simples des équations aux différences partielles de la Physique mathématique, *Journal de Mathématiques Pures et Appliquées*, **5**:5–20, 1879, http://eudml.org/doc/235258.
17. J.A. Méndez-Bermúdez, R. Aguilar-Sánchez, Dissipative fractional standard maps: Riemann–liouville and Caputo, *Chaos*, **35**(2):023114, 2025, https://doi.org/10.1063/5.0239987.
18. Z. Navickas, M. Ragulskis, A. Vainoras, R. Smidtaite, The explosive divergence in iterative maps of matrices, *Commun. Nonlinear Sci. Numer. Simul.*, **17**(11):4430–4438, 2012, https://doi.org/10.1016/j.cnsns.2012.03.018.
19. Z. Navickas, R. Smidtaite, A. Vainoras, M. Ragulskis, The logistic map of matrices, *Discrete Contin. Dyn. Syst., Ser. B*, **16**(3):927–944, 2011, https://doi.org/10.3934/dcdsb.2011.16.927.
20. U. Orinaite, I. Telksniene, T. Telksnys, M. Ragulskis, How does the fractional derivative change the complexity of the Caputo standard fractional map, *Int. J. Bifurcation Chaos Appl. Sci. Eng.*, **34**(07):2450085, 2024, https://doi.org/10.1142/S0218127424500858.

21. M. Ragulskis, Z. Navickas, The rank of a sequence as an indicator of chaos in discrete nonlinear dynamical systems, *Commun. Nonlinear Sci. Numer. Simul.*, **16**(7):2894–2906, 2011, https://doi.org/10.1016/j.cnsns.2010.10.008.

22. L. Ren, J. Wang, M. Fečkan, Asymptotically periodic solutions for caputo type fractional evolution equations, *Fract. Calc. Appl. Anal.*, **21**(5):1294–1312, 2018, https://doi.org/10.1515/fca-2018-0068.

23. F. Schilder, B.B. Peckham, Computing Arnold tongue scenarios, *J. Comput. Phys.*, **220**(2): 932–951, 2007, https://doi.org/10.1016/j.jcp.2006.05.041.

24. V.E. Tarasov, Differential equations with fractional derivative and universal map with memory, *J. Phys. A, Math. Theor.*, **42**(46):465102, 2009, https://doi.org/10.1088/1751-8113/42/46/465102.

25. V.E. Tarasov, Discrete map with memory from fractional differential equation of arbitrary positive order, *J. Math. Phys.*, **50**(12):122703, 2009, https://doi.org/10.1063/1.3272791.

26. V.E. Tarasov, *Fractional dynamics and discrete maps with memory*, pp. 409–453, Springer, Berlin, Heidelberg, 2010, https://doi.org/10.1007/978-3-642-14003-7_18.

27. V.E. Tarasov, From fractional differential equations with Hilfer derivatives: To discrete maps with memory, *Comput. Appl. Math.*, **40**(8):296, 2021, https://doi.org/10.1007/s40314-021-01674-5.

28. V.E. Tarasov, Integral equations of non-integer orders and discrete maps with memory, *Mathematics*, **9**(11):1177, 2021, https://doi.org/10.3390/math9111177.

29. V.E. Tarasov, Nonlinear fractional dynamics with kicks, *Chaos Solitons Fractals*, **151**:111259, 2021, https://doi.org/10.1016/j.chaos.2021.111259.

30. V.E. Tarasov, M. Edelman, Fractional dissipative standard map, *Chaos*, **20**(2):023127, 2010, https://doi.org/10.1063/1.3443235.

31. V.E. Tarasov, G.M. Zaslavsky, Fractional equations of kicked systems and discrete maps, *J. Phys. A, Math. Theor.*, **41**(43):435101, 2008, https://doi.org/10.1088/1751-8113/41/43/435101.

32. M.S. Tavazoei, A note on fractional-order derivatives of periodic functions, *Automatica*, **46**(5): 945–948, 2010, https://doi.org/10.1016/j.automatica.2010.02.023.

33. M.S. Tavazoei, M. Haeri, A proof for non existence of periodic solutions in time invariant fractional order systems, *Automatica*, **45**(8):1886–1890, 2009, https://doi.org/10.1016/j.automatica.2009.04.001.

34. J. Wang, M. Fečkan, Y. Zhou, Nonexistence of periodic solutions and asymptotically periodic solutions for fractional differential equations, *Commun. Nonlinear Sci. Numer. Simul.*, **18**(2):246–256, 2013, https://doi.org/10.1016/j.cnsns.2012.07.004.

35. D.H. Wolpert, W.G. Macready, No free lunch theorems for optimization, *IEEE Trans. Evol. Comput.*, **1**(1):67–82, 1997, https://doi.org/10.1109/4235.585893.

36. M. Yazdani, H. Salarieh, On the existence of periodic solutions in time-invariant fractional order systems, *Automatica*, **47**(8):1834–1837, 2011, https://doi.org/10.1016/j.automatica.2011.04.013.

37. G.M. Zaslavsky, *Hamiltonian Chaos and Fractional Dynamics*, Oxford Univ. Press, Oxford, 2005.